This is a repository copy of *Self-Assembly-Driven Electrospinning: The Transition from Fibers to Intact Beaded Morphologies*.

White Rose Research Online URL for this paper:
http://eprints.whiterose.ac.uk/121556/

Version: Accepted Version

Article:

Article Type (Communication)

Self-Assembly Driven Electrospinning: The Transition from Fibers to Intact Beaded Morphologies[a]

Linge Wang[1]*, Paul D. Topham[2], Oleksandr O. Mykhaylyk[3], Hao Yu[3], Anthony J. Ryan[3], J. Patrick A. Fairclough[3], Wim Bras[4]

────────

Prof. L. Wang, State Key Laboratory of Luminescent Materials and Devices, School of Materials Science and Engineering, South China University of Technology, Guangzhou 510640, China.
Email: lingewang@scut.edu.cn
Dr P. D. Topham, Chemical Engineering and Applied Chemistry, Aston University, Birmingham, B4 7ET, UK.
Dr O. O. Mykhaylyk, Dr H. Yu, Prof. A. J. Ryan, Prof. J. P. A. Fairclough, Department of Chemistry, University of Sheffield, Brook Hill, Sheffield, South Yorkshire, S3 7HF, UK. Dr H. Yu currently working at Beijing Advanced Materials Development Centre, Beijing, 100083, China. Prof. J. P. A. Fairclough currently working at Department of Mechanical Engineering, The University of Sheffield, Sheffield, S3 7HQ, UK
Dr W. Bras, DUBBLE CRG, ESRF, 6 rue Jules Horowitz, BP 220, F-38043, Grenoble Cédex 9, France.

────────

Polymer beads have attracted considerable interest for use in catalysis, drug delivery and photonics due to their particular shape and surface morphology. Electrospinning, typically used for producing nanofibers, can also be used to fabricate polymer beads if the solution has a sufficiently low concentration. In this work, we present a novel approach for producing more uniform, intact beads by electrospinning self-assembled block copolymer (BCP) solutions. This approach allows a relatively high polymer concentration to be used, yet with a low degree of entanglement between polymer chains due to microphase separation of the BCP in a selective solvent system. Herein, to demonstrate the technology, a well-studied polystyrene-poly(ethylene butylene)-polystyrene triblock copolymer has been dissolved in a

─────────────────

[a] **Supporting Information** is available online from the Wiley Online Library or from the author.

co-solvent system. The effect of solvent composition on the characteristics of the fibers and beads has been intensively studied, and the mechanism of this fiber-to-bead was found to be dependent on microphase separation of the BCP.

1. Introduction

Electrospinning is a relatively simple, efficient, and versatile method for fabricating continuous fibers from a variety of materials. Since the early 1990s, several research groups (most notably, Reneker and coworkers[1, 2]) have demonstrated the ability of electrospinning to fabricate ultrafine fibers. Electrospinning has attracted vast interest in research for potential application in diverse fields, such as tissue engineering,[3-7] drug delivery,[8-10] sensors,[11, 12] catalysis[13, 14] and fuel cells.[15, 16] One of the two main reasons for such wide ranging applications is that almost all polymers with sufficiently high molecular weight, including highly branched polymers,[17] can be prepared as ultrafine fibers using this simple technique.[18] Secondly, various, controllable surface morphologies and sizes of the electrospun products can be achieved with relative ease, such as smooth or rough surfaces, hollow[19] and porous[20, 21] morphologies, random or aligned fibers, and beads or beaded structures.[21, 22] The desired features can be obtained by adjusting the electrospinning parameters (applied voltage, polymer molecular weight, solution concentration, solution surface tension, solution conductivity, collecting method, etc.).[22-26] Beads (or beaded structures),[27] although often regarded as defects arising from the electrospinning process, have attracted significant attention for potential use in superhydrophobic surfaces,[22, 28] catalysis,[29] drug release systems,[30, 31] and photonic devices[32], due to their specific shapes, sizes and surface morphologies.[21, 33, 34] In order to understand the beaded structure, some studies have focused on the bead-to-fiber transition[27, 35] with respect to the rheological properties of polymer solutions, such as critical hydrodynamic concentration[36, 37] and chain entanglement.[38] Whilst the importance of chain entanglement is recognized, other solution properties, such as conductivity[39] and solvent evaporation,[35, 40] have also been investigated for their effects on the beaded structure and bead-to-fiber transition. In general, beads are fabricated from polymer solutions with low concentration or low molecular weight,[22] both of which produce a low degree of entanglement between polymer chains.[35]

In a different branch of so-called polymer nanotechnology, block copolymers (BCPs) are known to self-assemble into ordered phases with various periodic nanostructures, either in the bulk or in selective solvents, depending on the copolymer molecular weight, the relative volume fraction between the blocks and the interaction parameter between the disparate blocks (and solvent, if present).[41, 42] This phenomenon can be exploited to create physically-crosslinked three-dimensional networks, by using triblock copolymers.[43-45] Under certain conditions the end blocks can aggregate to form a micellar network structure, whilst the midblocks span, or bridge, the aggregated domains.[41, 46] However, if a suitable solvent system is employed, whereby the endblocks are solvated yet the midblocks favor aggregation, one can achieve a non-crosslinked micellar network at relatively high polymer concentration. Thus, electrospinning from such a self-assembled BCP solution, with a low degree of entanglement between the polymer chains, enables new bead morphologies to be accessed. These beaded morphologies differ from those typically accessed by low polymer concentration two main ways; (i) they remain intact following deposition and drying; and (ii) they are more uniform in terms of size distribution.

Herein, we discuss a novel approach to produce beads by 'electrospinning' from a self-assembled triblock copolymer solution in a selective solvent. A polystyrene-poly(ethylene butylene)-polystyrene (SEBS) triblock copolymer was dissolved in solvent mixtures of tetrahydrofuran (THF; a good solvent for both blocks) and N,N-dimethylformamide (DMF; a good solvent for the PS block only). In an attempt to study the fiber-to-bead transition, SEBS was dissolved in neat THF and electrospun into well-defined fibers. Subsequently, the morphological transition from fibers to beads could be observed by increasing the DMF content of the pre-spun polymer solution. The effect of solvent composition on the characteristics of the as-spun fibers and beads has been extensively studied, and the mechanism of this fiber-to-bead transition is discussed as a novel route to produce relatively uniform, intact polymer beads with a relatively narrow size distribution.

2. Experimental Section

2.1 Materials

Polystyrene-b-poly(ethylene butylene)-b-polystyrene (SEBS) triblock copolymer [M_n = 75.1 kg mol^{-1}, polystyrene (PS) volume fraction; ϕ = 0.30], also known as Kraton G1650, was obtained from Kraton Performance Polymers, Inc. PS homopolymer (M_n = 75.2 kg mol^{-1}) was obtained from Sigma-Aldrich (Fluka). THF and DMF (Laboratory Grade) were purchased from Fisher and used as received.

2.2 Electrospinning Experiments

The SEBS triblock copolymer and PS homopolymer were dissolved in THF at various concentrations (8-20 wt%) and in THF/DMF mixtures at various solvent compositions (THF/DMF from 100/0 to 0/100, w/w) with a fixed concentration of 14 wt%. All solutions were stored at 25 °C prior to use. All electrospinning experiments were performed at 25 °C in air using in-house apparatus similar to that described in the literature.[8, 47] A schematic of the electrospinning apparatus is shown in the Electronic Supporting Information (ESI), Figure S1. Each polymer solution was drawn into a 1 mL syringe connected to a 0.8 mm diameter flat-ended metallic needle. The solution was fed at 2 mL h^{-1} using a syringe pump (Aladdin-220, World Precision Instruments Ltd., USA) in a horizontal mount and the needle was connected to a high voltage supply (Genvolt-73030, Genvolt High Voltage Industries Ltd., UK), fixed at 20 kV. An aluminium drum (10 cm diameter) was earthed and used as a rotating collector, with the distance between the needle and collector edge being fixed at 15 cm. For analysis, the electrospun fibers and beads were dried under reduced pressure at room temperature for 24 hours to remove any residual solvent.

2.3 Characterization

Transmittance (turbidity) of the 14 wt% copolymer solutions at various THF:DMF compositions was measured by UV-Vis spectroscopy (Jasco UV-VIS 630) at 450 nm. Rheological properties were measured using a rheometer (AR-G2, TA instruments) with a concentric cylinder (Couette) fixture in oscillatory mode. All turbidity and viscosity measurements were performed at 25 °C. The surface morphologies of the polymer fibers or beads were revealed by scanning electron microscopy (SEM), using a Camscan Mk2 (operating at 15 kV for gold-coated samples). Average diameters of the fibers or beads produced from each solution were obtained using ImageJ software on all features from at least five SEM images. The self-assembled nanomorphologies of the triblock copolymer solutions were revealed via small-angle x-ray scattering (SAXS). SAXS measurements were performed at the European Synchrotron Radiation Facility (ESRF), Grenoble, France, on station BM26B (Dubble)[48] (wavelength of x-ray radiation, $\lambda = 1.24$ Å) over a q-range of 0.006 - 0.13Å^{-1} (modulus of the scattering vector q = $4\pi \sin\theta / \lambda$, where θ is half of the scattered angle) using a two-dimensional area detector (2D Pilatus 1M). Peak positions of wet rat-tail collagen were used to calibrate the q-axis. Some scattering experiments were also undertaken on a Bruker AXS NanoStar laboratory SAXS instrument equipped with a 2D position-sensitive gas detector (Hi-Star, Siemens AXS) and a Cu K$_\alpha$ radiation source ($\lambda = 1.54$ Å). Data were acquired over a q-range of 0.01 - 0.2 Å^{-1}. Two-dimensional (2D) SAXS patterns have been reduced to one-dimensional (1D) profiles by a standard procedure available either in the BSL software package or in the Bruker software supplied with the NanoStar. The 2D patterns, and their corresponding 1D profiles, have been subjected to incident beam intensity and background corrections.

3. Results and Discussion

Electrospinning from a self-assembled block copolymer (BCP) solution at high concentration, yet with a low degree of entanglement (due to microphase separation of the BCP in a selective

solvent environment), constitutes a novel approach to produce more uniform, intact beads. To this end, a co-solvent system of THF and DMF has been used to dissolve a SEBS triblock copolymer (Kraton, G1650) for electrospinning studies. DMF has a dielectric constant (or relative permittivity) higher than that of THF (36.7 versus 7.6, respectively[49]), and has a lower vapor pressure (2.7 kPa versus 21.6 kPa at 25 °C[49]). Generally, the THF/DMF mixed solvent system can be used to modify the diameter of electrospun fibers (due to differences in solution conductivity[22, 33, 50]) or surface morphology/porosity (due to differences in solvent vapour pressure[22, 51]).

Herein, the combination of THF and DMF with a SEBS triblock copolymer provides a unique opportunity to explore the shape morphology transition (fiber-to-bead) during electrospinning. The calculated Hansen's solubility parameters[52] of the solvent mixtures and the polymer blocks (Table S1, ESI) suggest that both PS and PEB blocks are almost fully soluble in THF/DMF at THF concentrations above 90 wt% [relative energy difference (RED) < 1, **Figure 1**] whereas the block copolymer is insoluble at THF concentrations below 65 wt% (RED > 1 for both blocks, Figure 1). These calculations are consistent with turbidity measurements of the copolymer in different THF/DMF compositions (Figure 1). Thus, THF/DMF compositions between 65 and 90 wt% THF (shaded area in Figure 1) represent a window for the THF/DMF-SEBS system where microphase separation of the copolymer is facilitated by the selective solubility of the copolymer blocks (RED < 1 for PS, but > 1 for PEB). In this work, the effect of selective solvent in a BCP solution on the morphology of electrospun assemblies has been studied in order to control the nanofeatures produced.

relative permittivity) higher than that of THF (36.7 versus 7.6, respectively[49]), and has a lower vapor pressure (2.7 kPa versus 21.6 kPa at 25 °C[49]). Generally, the THF/DMF mixed solvent system can be used to modify the diameter of electrospun fibers (due to differences in solution conductivity[22, 33, 50]) or surface morphology/porosity (due to differences in solvent vapour pressure[22, 51]).

Herein, the combination of THF and DMF with a SEBS triblock copolymer provides a unique opportunity to explore the shape morphology transition (fiber-to-bead) during electrospinning. The calculated Hansen's solubility parameters[52] of the solvent mixtures and the polymer blocks (Table S1, ESI) suggest that both PS and PEB blocks are almost fully soluble in THF/DMF at THF concentrations above 90 wt% [relative energy difference (RED) < 1, Figure 1] whereas the block copolymer is insoluble at THF concentrations below 65 wt% (RED > 1 for both blocks, Figure 1). These calculations are consistent with turbidity measurements of the copolymer in different THF/DMF compositions (Figure 1). Thus, THF/DMF compositions between 65 and 90 wt% THF (shaded area in Figure 1) represent a window for the THF/DMF-SEBS system where microphase separation of the copolymer is facilitated by the selective solubility of the copolymer blocks (RED < 1 for PS, but > 1 for PEB). In this work, the effect of selective solvent in a BCP solution on the morphology of electrospun assemblies has been studied in order to control the nanofeatures produced.

3.1. Morphology

THF is a good solvent for both the PS and PEB blocks of SEBS, while DMF is a selective solvent, only dissolving the PS endblocks. In order to identify an optimum working concentration to produce well-defined nanofibers, SEBS was dissolved in neat THF across a concentration range of 8 - 20 wt%. The SEM images (**Figure 2**a-f) show that at low concentration (≤ 10 wt%), due to the low viscosity and surface tension of the as-prepared solutions, beads were observed [average diameter 20.6 ± 6.8 μm for 8 wt% (see Figure S2a,

ESI) and 34.7 ± 14.0 μm for 10 wt%]. However, at 12 wt% and above, cylindrical fibers (average diameter approximately 9.3 ± 1.1 μm) were reproducibly fabricated until the viscosity of the solution became too high to electrospin (above 18 wt%). Consequently, 14 wt% was selected as an optimum polymer concentration for our study into the effect of microphase separation on electrospinning block copolymers. To this end, SEBS was dissolved in a range of THF/DMF mixtures (w/w: 100/0, 95/5, 90/10 and 80/20) at 14 wt% (see Figure 2d and g-i).

As the DMF content in the solvent mixture was increased, beads became favored over cylindrical fibers, even under the same operating conditions and polymer concentration (14 wt%). The fabricated beads were more uniform in size and shape than those produced from solutions of low concentration, with an average diameter of the spheres of approximately 7.9 (± 1.9) µm (see Figure S2b, ESI). In contrast, the beads produced via electrospraying from low concentration (< 12 wt%) in a single solvent (THF) had a much larger average diameter, around 20-30 µm, with a broader size distribution of the particles. Furthermore, the beads produced from solutions of low concentration appear collapsed/deformed (Figure S2a, ESI) whereas the beads produced from a self-assembled block copolymer solution appear largely intact (Figure S2b, ESI). Increasing the DMF content further (from 80/20 to 70/30) gave rise to macrophase separation due to poor solvent quality for the triblock copolymer (see Figure S3, ESI) and could not be processed into beads or fibres. The turbidity measurements (Figure 1) reflect this, clearly showing a loss of transmittance at 70/30 (and progressively higher DMF contents).

3.2. Mechanism

These findings are somewhat different to those observed when electrospinning homopolymers from solvent mixtures.[22, 35, 51, 56, 57] The observations herein indicate that there is a different mechanism in play when processing from a mixture of solvents for BCPs than there is for

homopolymers. Mixed solvent systems give rise to polymer solutions with varying important properties in electrospinning, such as conductivity and viscosity. However, when a BCP is introduced to a solvent mixture where one of the solvents shows selectivity (preferential solubility for one of the blocks), the changes in conductivity and/or viscosity are significantly masked by the presence of microphase separation. In the SEBS/selective solvent solution, the conductivity increased with DMF content (see Figure S4, ESI), yet the size of the beads (Figure S2b) is similar to that of the fibers (Figure 2d) with the same SEBS concentration but with vastly different conductivity. In contrast, commonly, fiber diameter deceases with increase in DMF content for both homopolymers[22] and BCPs[17] in THF/DMF co-solvent systems, provided that there is no phase separation in those pre-spun solutions.

For the SEBS block copolymer, as aforementioned, THF is a good solvent for both PS and PEB blocks. However, DMF, and therefore solvent mixtures containing sufficient quantities of DMF, show selectivity for PS (see Table S1, ESI). Thus, the entanglement between polymer chains is reduced on increasing DMF content as the block copolymer microphase separates to form various self-assembled nanomorphologies. These speculations, based on calculated Hansen's solubility parameters and turbidity measurements (Table S1 and Figure 1), have been confirmed by small angle x-ray scattering (SAXS, **Figure 3**). The nanostructure within the copolymer solution transforms as the ratio of THF/DMF is varied. Starting with THF alone, at 14 wt%, SAXS analysis reveals only a weak structural peak arising from the solution. This peak, considering liquid-like behavior of the solution (Figure S5, ESI), can be associated with copolymer chain interactions typically observed for concentrated polymer solutions. This peak evolves into a pronounced structural peak at higher concentrations of SEBS (Figure S6, ESI) indicating the formation of structural domains due to both aggregation and self-separation of copolymer chains. When a small amount of DMF is added (THF/DMF = 95/5), the block copolymer remains soluble in the solvent mixture (Figure S5, ESI) and demonstrates similar structural behaviour (Figures 3 and S7). However, when the DMF

concentration reaches 10 wt% (THF/DMF = 90/10), at the theoretical point where DMF should act selectively on the copolymer blocks (RED > 1, Figure 1), a sharp diffraction peak appears in the SAXS pattern (Figure 3) indicating that a structural transition takes place in the sample. This transition is also detected by a sharp increase in the solution viscosity (Figure S5, ESI). A well-ordered structure, revealed by a number of diffraction peaks, is observed for a copolymer solution of THF/DMF 80/20, approximately corresponding to the centre of the DMF concentration interval where the mixed solvent is expected to act selectively on PS (Figure 3). It was found that the relative positions of the first four resolved diffraction peaks ($q/q^* = 1$, 1.14, 1.63 and 1.88, where q^* is the first peak position) correspond to a face-centred cubic (FCC) structure. Moreover, the entire diffraction pattern was also consistent with an FCC structure (see Figure 3b for Miller indices). Thus, when the solvent media becomes poorer for the PEB block, self-assembly of SEBS occurs into an FCC structure. According to the SAXS data, the lattice period is approximately 78 nm (obtained by a least square fit to the values of the lattice period calculated from the position of the first four peaks of the indexed diffraction pattern). It is noticeable from the SAXS pattern that the 113 peak is significantly weakened and the 222 and 044 peaks are absent. These observations can be attributed to overlap of the 113 and 222 peaks with the position of the first minimum of the spherical micelle form factor, whereas the 044 peak overlaps with the position of the second minimum of the spherical micelle form factor. Thus, q values of the first- and second minima of the micelle form factor, estimated from the SAXS pattern should be approximately 0.27 nm^{-1} and 0.45 nm^{-1}, respectively. Considering that q values of the minima of the spherical form factor are related to the sphere radius as $qR = 4.49$ (for the first minimum) and $qR = 7.73$ (for the second minimum), the sphere diameter (2R) can be calculated to be approximately 33 nm ($= 2 \times 4.49 / 0.27$ nm^{-1} or $= 2 \times 7.73 / 0.45$ nm^{-1}). Assuming that the FCC structure formed by micelles can be represented as PEB blocks embedded in a PS matrix (Figure 4b) the obtained value should correspond to the PEB micelle core diameter.

For bulk SEBS copolymer, at room temperature, the PS chains constitute glassy domains, whereas the PEB midblock chains form bridges between PS end blocks, creating an ordered network.[58-60] In a selective solvent for PEB, similarly, the PS blocks aggregate into discrete domains to create evenly distributed physical crosslinks between the midblock (PEB) chains.[61] The PEB blocks form either loops, starting and ending within the same PS core, or bridges between different PS domains (see **Figure 4**a). However, in the case of a selective solvent for the endblocks (PS), typically, core-corona structured micellar aggregates (gels) [61] are formed (a non-crosslinked micellar network), in which the endblocks (PS) are solvated yet the midblocks (PEB) favor aggregation. Micellar formation is caused by a thermodynamically driven reduction in enthalpy by the minimization of direct contact between the midblock chains and the solvent.[46] Different characteristics can be expected SEBS in solvent systems that are selective for the middle (PEB) block (Figure 4b). In this non-crosslinked micellar network (at THF/DMF = 80/20), the degree of entanglement of the plasticized PS chains is much lower than when completely dissolved in THF. Consequently, beads were fabricated when electrospinning SEBS from a selective solvent system (THF/DMF = 80/20). Importantly, the beads produced in this manner are more uniform and intact, attributed to the PEB chains being aggregated into hard, globular cores prior to spinning, with less solvent evaporation taking place during the formation of the beads. In contrast, the beads electrospun from the SEBS solution (in pure THF) at low concentration were formed following a higher extent of solvent evaporation from polymer chains in an expanded coil state, resulting in collapsed or defected morphologies.

As a controlled experiment, a similar molecular weight PS homopolymer sample was dissolved in THF/DMF at 100/0, 90/10 and 80/20, at fixed concentrations of 14 wt% and 20 wt%. It was shown that no such "fiber-to-bead" transition was observed when increasing the DMF content (see Figures S8 and S9, ESI). In contrast, there was a tendency of an opposing transition, with "beads-to-fibers" observed due to the increasing surface tension and viscosity

of the solution with increasing DMF content.[22, 33, 35, 51, 56, 57] These results prove that the beads produced from our SEBS solution in a selective solvent system (THF/DMF = 80/20) are driven by the self-assembly (microphase separation) of the SEBS block copolymer.

4. Conclusions

In summary, we have demonstrated a novel approach to produce beads by electrospinning from self-assembled BCP solutions. A SEBS triblock copolymer was dissolved in a co-solvent system of THF/DMF at varying solvent compositions to alter the selective solubility of the disparate polymer blocks. It was found that the morphological transition from fibers to beads took place on increasing the DMF content in the mixture. SAXS and turbidity measurements, alongside theoretical solubility parameter calculations, showed that one can pass through three regimes as the ratio is altered in a THF/DMF co-solvent system; the block copolymer is almost fully soluble when THF > 90 wt%, self-assembled (microphase separation) when 90 wt% > THF > 65 wt% and insoluble (macrophase separation) when THF < 65 wt%. Interestingly, an ordered FCC micellar network structure was formed in THF/DMF at 80/20. The beads produced from the self-assembled block copolymer are completely different from the beads conventionally generated in electrospraying by lowering the polymer concentration; the former are smaller, intact and display a more uniform size distribution.

Supporting Information

Supporting Information is available from the Wiley Online Library or from the author ((delete if necessary))

[1] J. Doshi, D. H. Reneker, J Electrostat **1995**, 35, 151.

[2] D. H. Reneker, I. Chun, Nanotechnology **1996**, 7, 216.

[3] M. Rampichova, J. Chvojka, M. Buzgo, E. Prosecka, P. Mikes, L. Vyslouzilova, D. Tvrdik, P. Kochova, T. Gregor, D. Lukas, E. Amler, Cell Proliferation **2013**, 46, 23.

[4] L. A. S. Callahan, S. B. Xie, I. A. Barker, J. K. Zheng, D. H. Reneker, A. P. Dove, M. L. Becker, Biomaterials **2013**, 34, 9089.

[5] F. Lin, J. Y. Yu, W. Tang, J. K. Zheng, S. B. Xie, M. L. Becker, Macromolecules **2013**, 46, 9515.

[6] C. Wang, M. Wang, Front. Mater. Sci. **2014**, 8, 3.

[7] H. S. Kim, H. S. Yoo, Nanomedicine **2014**, 9, 517.

[8] L. G. Wang, M. Wang, P. D. Topham, Y. Huang, RSC Adv. **2012**, 2, 2433.

[9] R. Krishnan, S. Sundarrajan, S. Ramakrishna, Macromol Mater Eng **2013**, 298, 1034.

[10] X. L. Hu, S. Liu, G. Y. Zhou, Y. B. Huang, Z. G. Xie, X. B. Jing, J Control Release **2014**, 185, 12.

[11] B. Ding, M. R. Wang, X. F. Wang, J. Y. Yu, G. Sun, Mater Today **2010**, 13, 16.

[12] X. F. Wang, F. H. Cui, J. Y. Lin, B. Ding, J. Y. Yu, S. S. Al-Deyab, Sens. Actuator B-Chem. **2012**, 171, 658.

[13] L. F. Yin, J. F. Niu, Z. Y. Shen, Y. P. Bao, S. Y. Ding, Mater Lett **2011**, 65, 3131.

[14] G. D. Nie, S. K. Li, X. F. Lu, C. Wang, Chem J Chinese U **2013**, 34, 15.

[15] S. Agarwal, A. Greiner, J. H. Wendorff, Prog Polym Sci **2013**, 38, 963.

[16] J. G. Lee, J. H. Park, Y. G. Shul, Nature Communications **2014**, 5, 10.

[17] L. Wang, C. M. Li, A. J. Ryan, S. P. Armes, Adv Mater **2006**, 18, 1566.

[18] Z. M. Huang, Y. Z. Zhang, M. Kotaki, S. Ramakrishna, Compos Sci Technol **2003**, 63, 2223.

[19] D. Li, A. Babel, S. A. Jenekhe, Y. N. Xia, Adv Mater **2004**, 16, 2062.

[20] S. Megelski, J. S. Stephens, D. B. Chase, J. F. Rabolt, Macromolecules **2002**, 35, 8456.

[21] G. Eda, S. Shivkumar, J Mater Sci **2006**, 41, 5704.

[22] J. F. Zheng, A. H. He, J. X. Li, J. A. Xu, C. C. Han, Polymer **2006**, 47, 7095.

[23] X. H. Zong, K. Kim, D. F. Fang, S. F. Ran, B. S. Hsiao, B. Chu, Polymer **2002**, 43, 4403.

[24] M. Bognitzki, W. Czado, T. Frese, A. Schaper, M. Hellwig, M. Steinhart, A. Greiner, J. H. Wendorff, Adv Mater **2001**, 13, 70.

[25] S. L. Zhao, X. H. Wu, L. G. Wang, Y. Huang, J Appl Polym Sci **2004**, 91, 242.

[26] S. A. Theron, E. Zussman, A. L. Yarin, Polymer **2004**, 45, 2017.

[27] H. Fong, I. Chun, D. H. Reneker, Polymer **1999**, 40, 4585.

[28] Y. Il Yoon, H. S. Moon, W. S. Lyoo, T. S. Lee, W. H. Park, J Colloid Interf Sci **2008**, 320, 91.

[29] C. C. Zhang, X. Li, T. Zheng, Y. Yang, Y. X. Li, Y. Li, C. Wang, L. J. Li, Desalin Water Treat **2012**, 45, 324.

[30] S. Somvipart, S. Kanokpanont, R. Rangkupan, J. Ratanavaraporn, S. Damrongsakkul, Int J Biol Macromol **2013**, 55, 176.

[31] R. Sridhar, R. Lakshminarayanan, K. Madhaiyan, V. Amutha Barathi, K. H. C. Lim, S. Ramakrishna, Chem Soc Rev **2015**, 44, 790.

[32] N. Tomczak, N. F. van Hulst, G. J. Vancso, Macromolecules **2005**, 38, 7863.

[33] K. H. Lee, H. Y. Kim, H. J. Bang, Y. H. Jung, S. G. Lee, Polymer **2003**, 44, 4029.

[34] J. T. Chen, W. L. Chen, P. W. Fan, I. C. Yao, Macromol Rapid Comm **2014**, 35, 360.

[35] G. Eda, S. Shivkumar, J Appl Polym Sci **2007**, 106, 475.

[36] M. G. McKee, G. L. Wilkes, R. H. Colby, T. E. Long, Macromolecules **2004**, 37, 1760.

[37] P. Gupta, C. Elkins, T. E. Long, G. L. Wilkes, Polymer **2005**, 46, 4799.

[38] S. L. Shenoy, W. D. Bates, H. L. Frisch, G. E. Wnek, Polymer **2005**, 46, 3372.

[39] K. H. Lee, H. Y. Kim, Y. M. La, D. R. Lee, N. H. Sung, J Polym Sci Pol Phys **2002**, 40, 2259.

[40] G. Larsen, R. Spretz, R. Velarde-Ortiz, Adv Mater **2004**, 16, 166.

[41] L. Leibler, Macromolecules **1980**, 13, 1602.

[42] M. W. Matsen, F. S. Bates, Macromolecules **1996**, 29, 1091.

[43] J. R. Howse, P. Topham, C. J. Crook, A. J. Gleeson, W. Bras, R. A. L. Jones, A. J. Ryan, Nano Lett **2006**, 6, 73.

[44] P. D. Topham, J. R. Howse, C. J. Crook, A. J. Gleeson, W. Bras, S. P. Armes, R. A. L. Jones, A. J. Ryan, Macromol Symp **2007**, 256, 95.

[45] P. D. Topham, J. R. Howse, C. M. Fernyhough, A. J. Ryan, Soft Matter **2007**, 3, 1506.

[46] P. D. Topham, J. R. Howse, O. O. Mykhaylyk, S. P. Armes, R. A. L. Jones, A. J. Ryan, Macromolecules **2006**, 39, 5573.

[47] C. Z. Chen, L. G. Wang, Y. Huang, Applied Energy **2011**, 88, 3133.

[48] W. Bras, I. P. Dolbnya, D. Detollenaere, R. van Tol, M. Malfois, G. N. Greaves, A. J. Ryan, E. Heeley, J. Appl. Crystallogr. **2003**, 36, 791.

[49] I. M. Smallwood, "Handbook of Organic Solvent Properties", Arnold/Halsted Press, UK, 1996.

[50] L. Wang, P. D. Topham, O. O. Mykhaylyk, J. R. Howse, W. Bras, R. A. L. Jones, A. J. Ryan, Adv Mater **2007**, 19, 3544.

[51] J. Y. Lin, B. Ding, J. Y. Yu, Y. Hsieh, ACS Appl. Mater. Interfaces **2010**, 2, 521.

[52] C. M. Hansen, "Hansen Solubility Parameters: A User's Handbook, Second Edition", CRC Press, Boca Raton, 2007, p. 519.

[53] A. Haque, E. R. Morris, Carbohyd Polym **1993**, 22, 161.

[54] A. Clark, S. Ross-Murphy, "Structural and mechanical properties of biopolymer gels", in Biopolymers, Springer Berlin Heidelberg, 1987, p. 57.

[55] H. Winter, M. Mours, "Rheology of Polymers Near Liquid-Solid Transitions", in Neutron Spin Echo Spectroscopy Viscoelasticity Rheology, Springer Berlin Heidelberg, 1997, p. 165.

[56] L. Wannatong, A. Sirivat, P. Supaphol, Polym Int **2004**, 53, 1851.

[57] T. Uyar, F. Besenbacher, Polymer **2008**, 49, 5336.

[58] N. Mischenko, K. Reynders, K. Mortensen, R. Scherrenberg, F. Fontaine, R. Graulus, H. Reynaers, Macromolecules **1994**, 27, 2345.

[59] A. Arevalillo, M. E. Munoz, A. Santamaria, L. Fraga, J. A. Barrio, Eur Polym J **2008**, 44, 3213.

[60] J. H. Laurer, R. Bukovnik, R. J. Spontak, Macromolecules **1996**, 29, 5760.

[61] K. Mortensen, E. Theunissen, R. Kleppinger, K. Almdal, H. Reynaers, Macromolecules **2002**, 35, 7773.
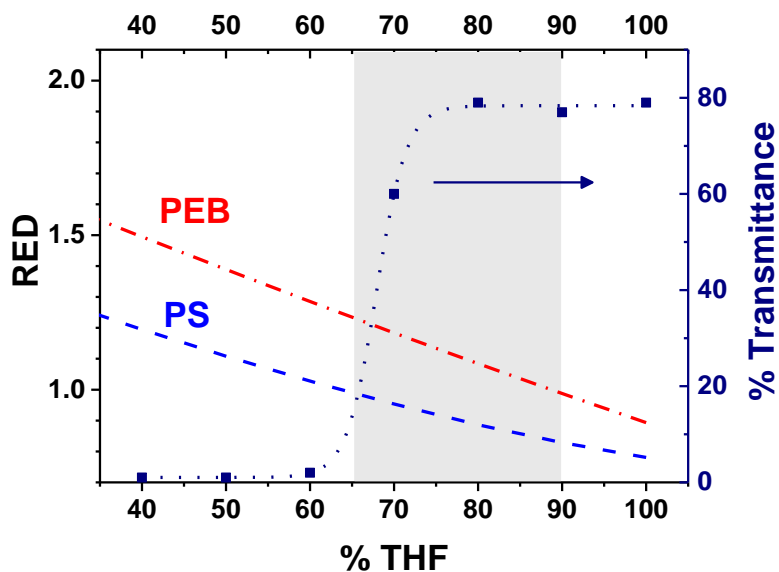
Figure 1. The relative energy difference (RED) of polystyrene (PS, blue dashed line) and poly(ethylene-butylene) (PEB, red dash-dotted line) calculated from Hansen solubility parameters of the polymers and turbidity measurements of the 14 wt% SEBS block copolymer solutions (■) in THF/DMF solvent mixtures (see Table S1, ESI). The navy dotted line shows a Boltzman fit to the turbidity measurements.
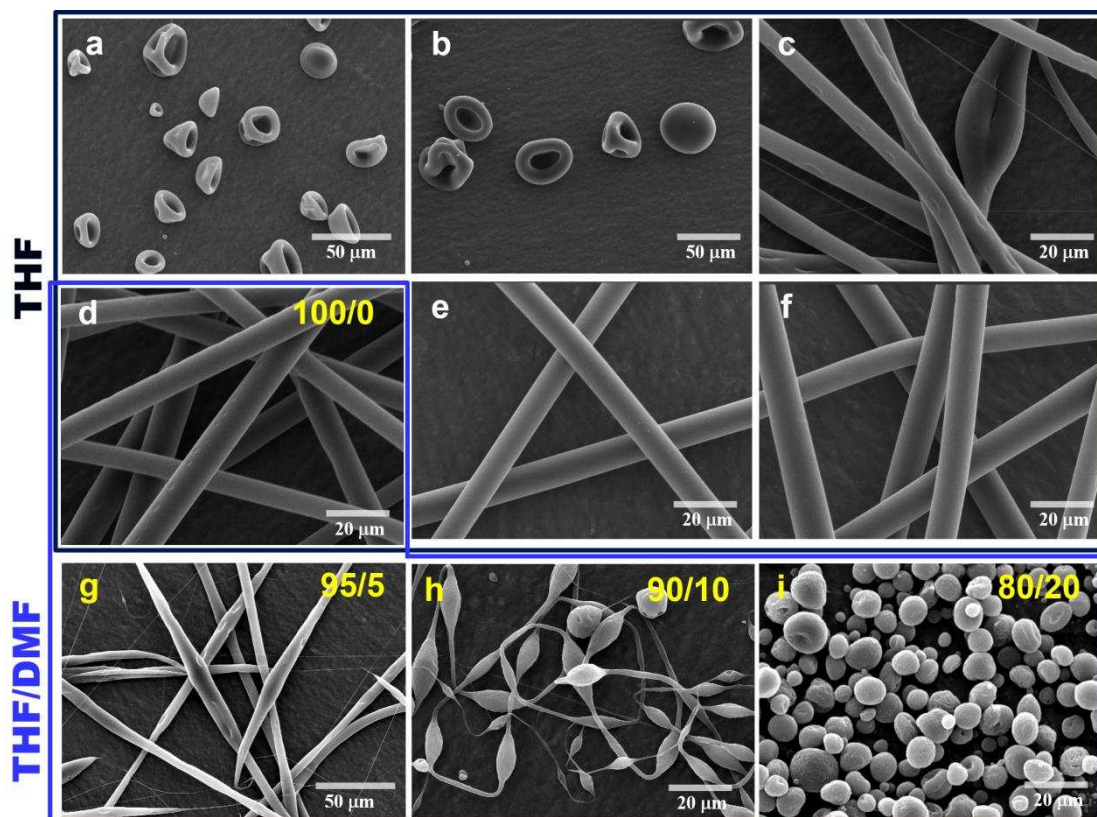

Figure 2. SEM images of electrosprayed beads (a and b) and electrospun fibers (c – f) of SEBS from neat THF solutions at varying polymer concentrations (8 wt%, 10wt%, 12 wt%, 14wt%, 16 wt% and 18wt% for a - f, respectively). SEM images (d, g-i) show the effect of

solvent composition (THF/DMF) on the morphology of electrically-processed SEBS solutions at 14 wt% (THF/DMF = 100/0, 95/5, 90/10 and 80/20, for d, g, h and i, respectively).
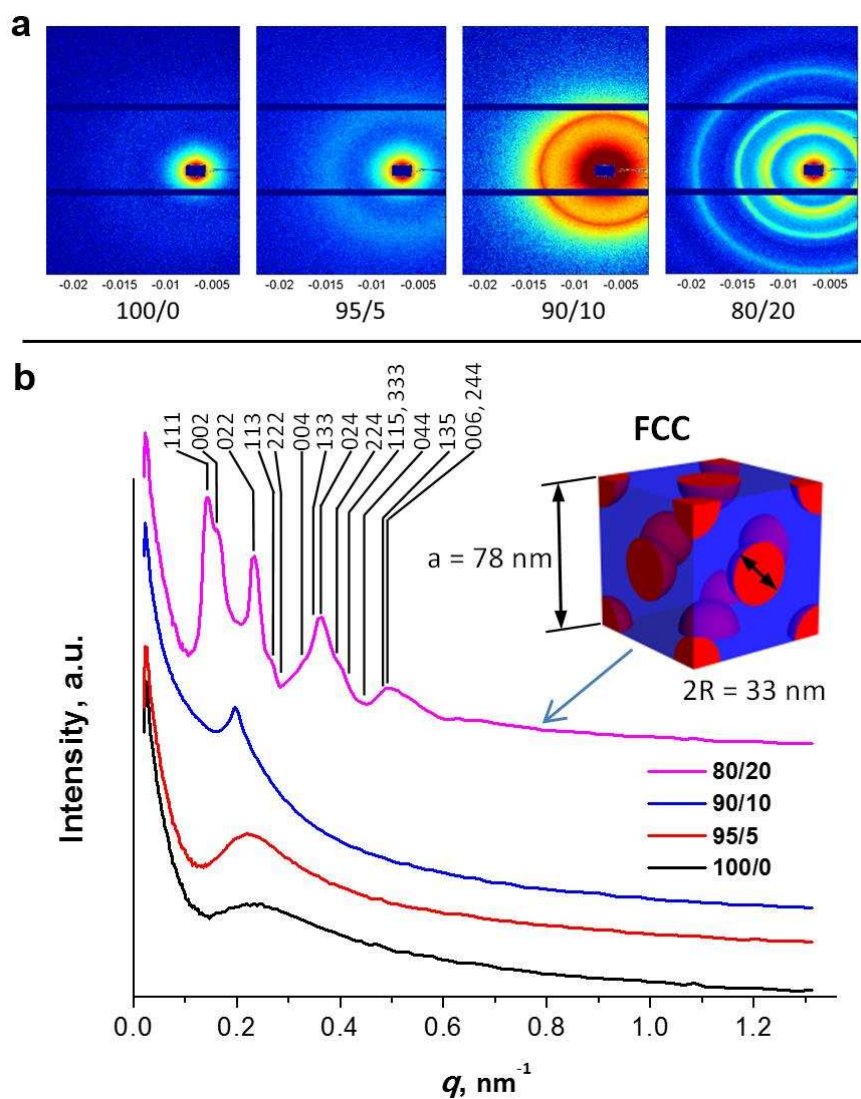

Figure 3. Small angle x-ray scattering data of the 14wt% SEBS solutions at different THF/DMF ratios, where (a) shows the 2D SAXS images and (b) shows the corresponding 1D data of intensity versus q.
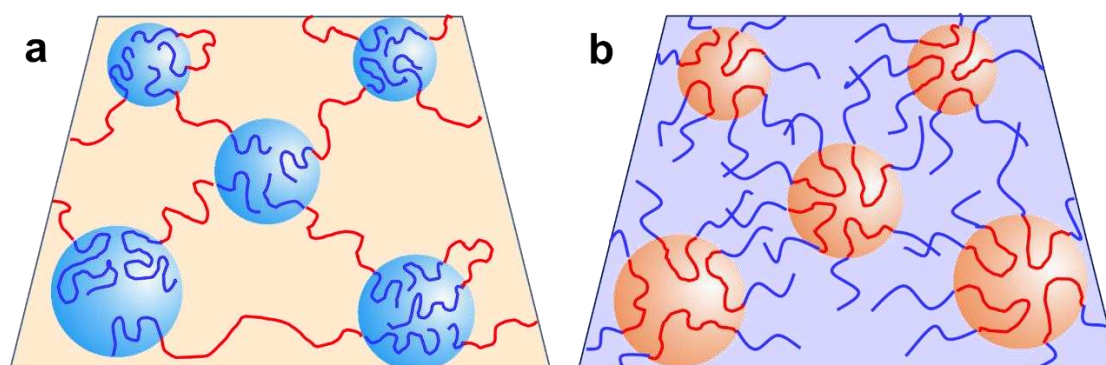
Figure 4. Schematic illustration of the SEBS network structure: (a) in a selective solvent for PEB that forms a gel network and (b) in a selective solvent for PS that forms a non-crosslinked micellar network and leads to intact beaded morphologies presented herein. PS chains are depicted in blue and PEB chains are in red.

A novel approach for producing more uniform, intact beads by electrospinning a self-assembled block copolymer (BCP) solution is demonstrated. This approach allows a relatively high polymer concentration to be used, yet with a low degree of entanglement between polymer chains due to microphase separation of the BCP in a selective solvent system.

Linge Wang[1]*, Paul D. Topham[2], Oleksandr O. Mykhaylyk[3], Hao Yu[3], Anthony J. Ryan[3], J. Patrick A. Fairclough[3], Wim Bras[4]

Self-Assembly Driven Electrospinning: The Transition from Fibers to Intact Beaded Morphologies